Electronic Supplementary Material (ESI) for Journal of Materials Chemistry A.

Supporting Information for

Advanced N-doped Mesoporous Molybdenum Disulfide Nanosheets and the Enhanced Lithium-Ion Storage Performance

Si Qin, Weiwei Lei*, Dan Liu, and Ying Chen*

Institute for Frontier Materials, Deakin University, 75 Pigdons Rd, Waurn Ponds,
Victoria 3216, Australia

E-mail: weiwei.lei@deakin.edu.au, ian.chen@deakin.edu.au

Experimental Section

Synthesis: About 0.5 g molybdenum chloride ($MoCl_5$, Aldrich, 99%) and 1.67 g thiourea ($(NH_2)_2CS$, Alfa-Aesar, 99%), equivalent to a molar ratio of 1:12, were first dissolved in ethanol forming a brownish red solution under stirring. The solution was allowed to dry in a fume hood under intensive stirring resulting in a brown powder, the process usually takes around 2 days. The powders were collected and placed in a quartz boat and heated in a tube furnace at 600 °C for three hours with a ramp rate of 10 °C min^{-1} under a 0.1 L min^{-1} argon flow. The product was collected after the furnace cooled down naturally. For comparison purpose, non-doped MoS_2 nanosheets were prepared by exfoliation of bulk MoS_2 following a method reported elsewhere.[1]

Characterization: X-ray diffraction (XRD) analysis was performed with a Panalytical X'Pert Pro using Cu Kα radiation source with 2θ range of 10-80° and a step size of 0.02°. The thermal behaviour of the precursor was analysed using thermogravimetric analysis (TGA) on a Netzsch STA 409 PC/PG thermal analyser at a heating rate of 10 K min^{-1} from room temperature to 1000 °C in argon gas flow. Scanning electron microscopy (SEM) was conducted using a Carl Zeiss Supra. The atomic force microscopy (AFM) measurements were performed on a Cypher atomic force microscope. Samples were ultrasonicated and dispersed in water, and the dispersion were dropped on mica substrate for AFM analysis. Transmission electron microscopy (TEM) images, Energy filtered TEM (EFTEM) and energy-dispersive X-ray spectroscopy (EDS) element mapping were taken on a JEOL JEM-2100 at an acceleration voltage of 200 kV. Nitrogen adsorption and desorption isotherm was obtained using a Tristar 3000 apparatus at 77K. X-ray photoelectron spectra (XPS) were acquired on a Kratos AXIS Nova with Al Kα X-ray source. Raman spectra were obtained under ambient conditions on a Renishaw inVia confocal Raman microscope using 514.5 nm laser line from an Ar ion laser. To avoid heating and damaging of the sample, the power of the laser radiation was always kept below 1 mW. The Si Raman band at 520 cm^{-1} was used as an internal frequency calibration reference. To compare the conductivity, sample were prepared as films. Samples were first dispersed in N-Methyl-2-pyrrolidone (NMP) by ultrasonication. The dispersion were filtrated through a 0.2 μm filter membrane and dried overnight in a vacuum oven. The thickness of the films can be measured by SEM analysis of the cross section. The films were cut into square shape and two electrodes were prepared by sputtering silver on the sides. The conductivity can be deduced from the IV curve of the film. Each test were repeated on three different film prepared separately to make sure the results are repeatable.

Electrochemical measurements: Coin-type cells were assembled in an argon-filled glove-box, with both moisture and oxygen levels less than 1 ppm. Active material (N-MoS_2 nanosheets), conductivity agent (Super P carbon black, Timcal) and polyvinylidine difluoride binder (PVDF, Aldrich) were mixed with a weight ratio of 80:10:10 in N-Methylpyrrolidone (NMP, Aldrich) solvent to produce a slurry. The working electrodes were prepared by coating the slurry onto copper foil current collector and then dried in a vacuum oven to completely remove the solvent and water. Electrodes with MoS_2 particles as active material were prepared by the same procedure described above. Lithium foil was used as the counter and reference electrode, and 1M $LiPF_6$ in 1:1 v/v ethylene carbonate (EC) and diethyl carbonate (DEC) was used as electrolyte. Galvanostatic tests were carried out on Land CT2001A battery testing system and the working electrodes were cycled between 3 V and 0.01 V vs. Li^+/Li. Electrochemical impedance spectroscopy (EIS) was acquired with a Solartron 1470E potentiostat and 1255B frequency response analyser setup with a polarization potential of 10 mV in a frequency range of 10 kHz – 10^{-2} Hz. EIS measurements were carried out after 10 cycles.

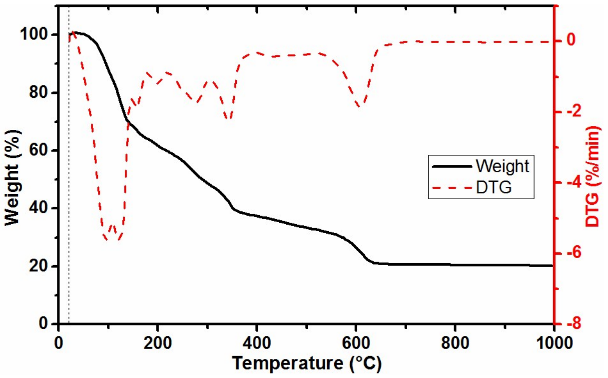

Figure S1. TGA curve of the precursor

TGA results (Figure S1) from the precursor can be divided into four parts. The first stage of the weight lost started almost right after the heating started. The TGA curve shows a steep weight lost cliff from the start to 130 °C, which can be attributed to the evaporation of the remaining ethanol and water in the sample. The second stage is where the starting materials begin to melt and decompose. Thiourea decomposes at a temperature range from 187 to 246 °C giving out various gases including NH_3, HNCS, CS_2 according to literature, leading to a ~80% of weight lost.[2] The gases released by thiourea decomposition create gas bubbles and agitate the reaction medium. The gas/liquid interface could also provide a site for the formation of MoS_2. The nitrogen containing gases are essential for the subsequent formation of N-doped MoS_2. The third stage shows a gentle slope from 350 °C and goes up to 620 °C. This stage is crucial to the formation and crystallization of MoS_2, as it has been reported sample synthesised at 350 °C has a disordered or amorphous structure, which suggests low temperature annealing is not suitable for the growth of MoS_2.[3] There is almost no weight lost after

620 °C. There is almost no weight lost after 620°C. Therefore, the TGA result suggest that the MoS_2 nanosheets were formed during 350°C-620 °C, and N was doped simultaneously due to the NH_3 and HNCS gases releasing.

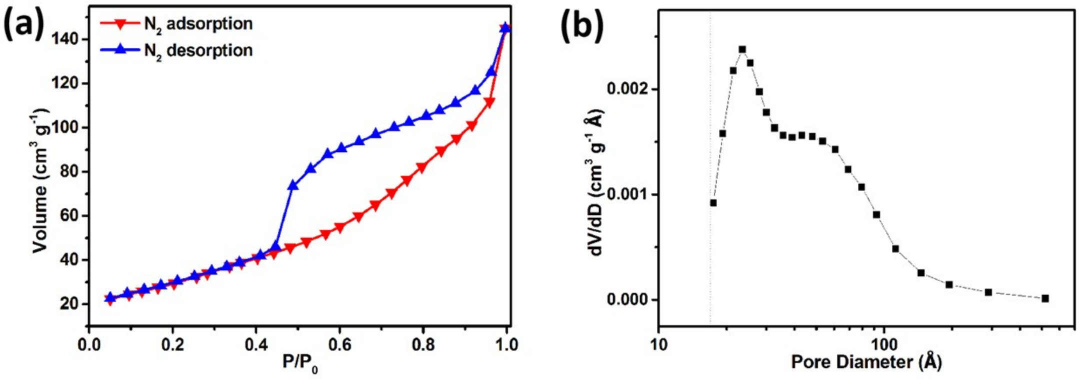

Figure S2. (a) Nitrogen adsorption/desorption isotherm of the product. (b) Barrett-Joyner-Halenda (BJH) pore size distribution of the product calculated from the nitrogen desorption result.

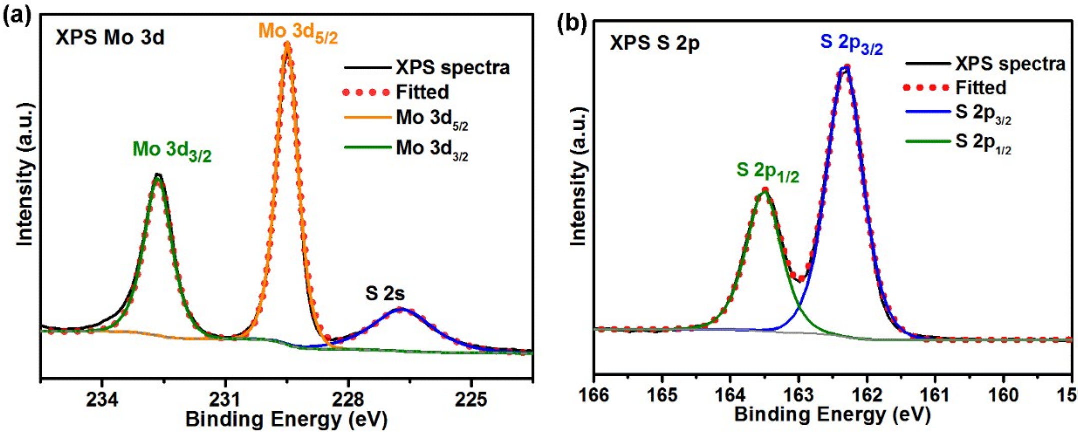

Figure S3. (a) XPS spectra of the Mo 3d region (b) XPS spectra of the S 2p region.

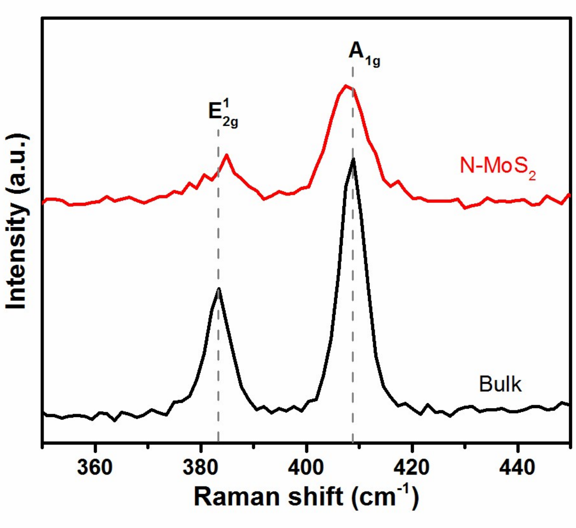

Figure S4. Raman spectra of bulk MoS_2, and N-doped MoS_2 nanosheets, acquired using 514.5 nm laser line.

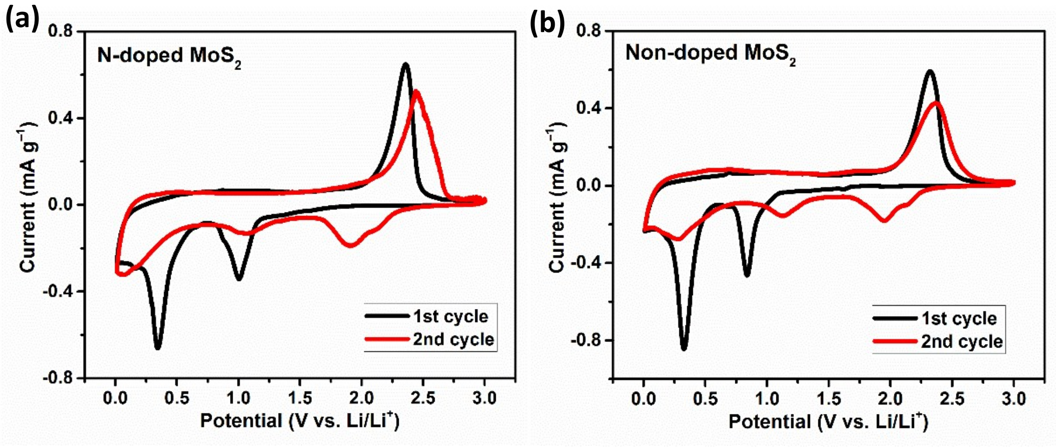

Figure S5. Cycling voltammetry (CV) curves of the N-MoS_2 nanosheets and non-doped MoS_2 nanosheets of the first two cycles, scan rate 0.1 mV s^{-1}.

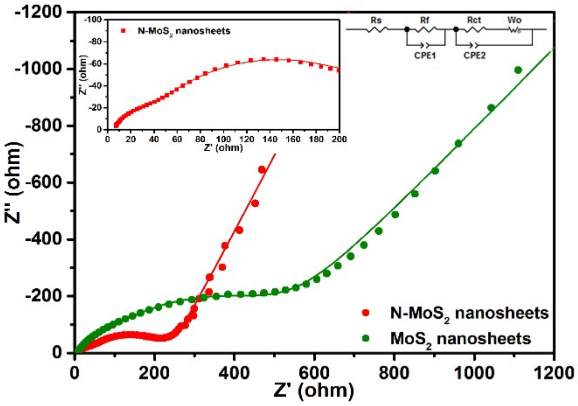

Figure S6. Nyquist plots of the electrochemical impedance spectrum of the N-MoS_2 nanosheets and non-doped MoS_2 nanosheets, inset showing the high frequency area of the plot and the equivalent circuit used for fitting.

The two compressed semicircles in Nyquist plots can be assigned to the electrode/electrolyte interface resistance (Rf) and capacitance (CPE1), and charge transfer resistance (Rct) and the double layer capacitance (CPE2), respectively. The inclined line in the low frequency region is assigned to the Warburg impedance (Wo) representing Li^+ ion diffusion in electrode material.

The diffusion coefficient of lithium ions could be calculated from the low frequency range according to the following equation:[2]

$$D= R^2T^2/2A^2n^4F^4C^2\sigma^2$$

where R is the gas constant, T is the absolute temperature, A is the surface area of the cathode, n is the number of electrons per molecule during oxidization, F is the Faraday constant, C is the lithium ion concentration in electrode material, and σ is the Warburg factor which is relative with Z'.

$$Z'=R_D+R_L+ \sigma\omega^{1/2}$$

Figure S7. SEM image of typical MoS_2 particles.

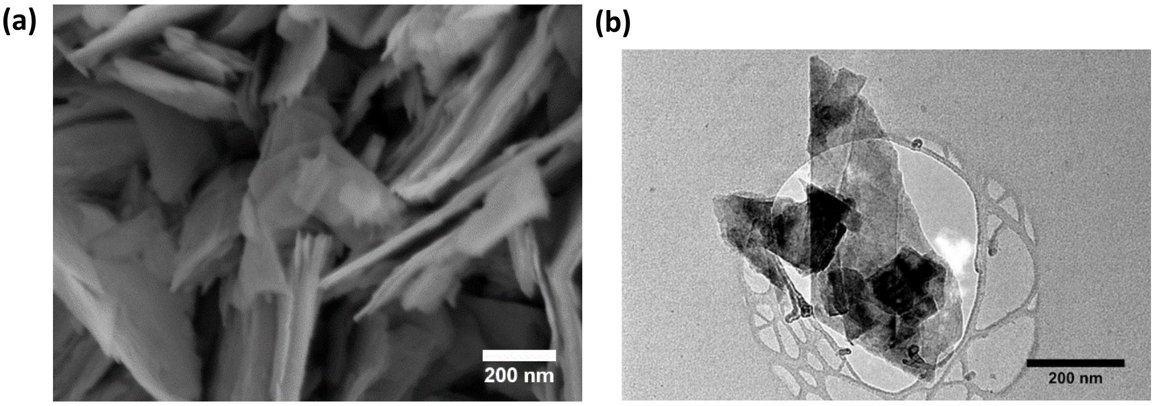

Figure S8. (a) SEM and (b) TEM images of typical non-doped MoS_2 nanosheets.

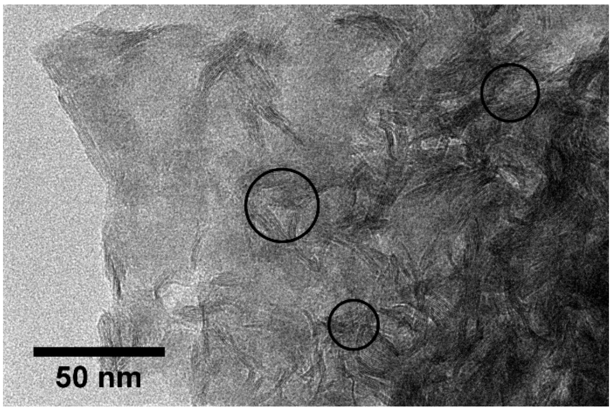

Figure S9. TEM images showing typical interconnected and aggregated N-MoS_2 nanosheets and the porous structure, the marked areas are spaces encircled by several nanosheets.

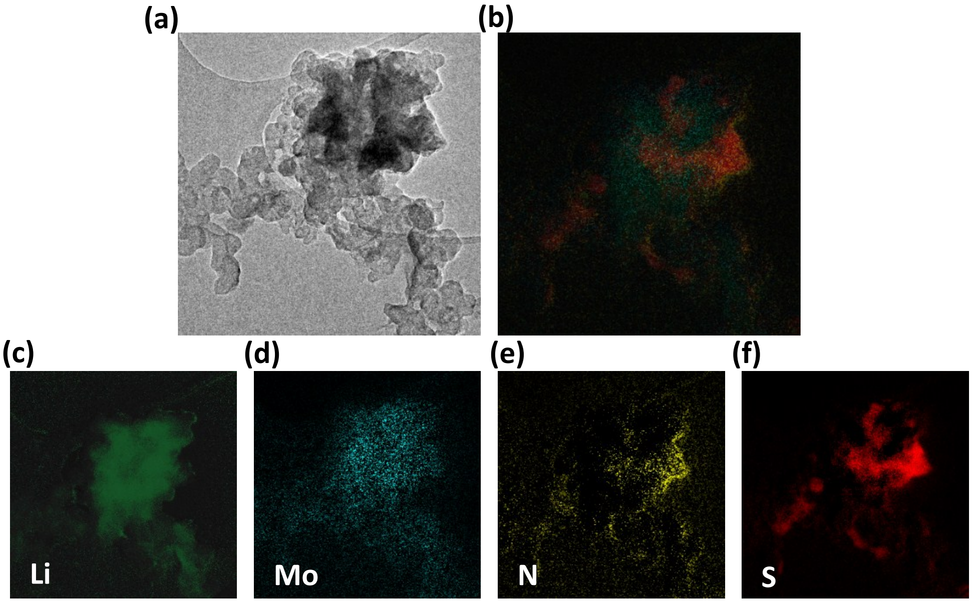

Figure S10. Energy filtered TEM (EFTEM) element map showing distribution of (a) bright field TEM image, (b) combined element map, (c) Li, (d) Mo, (e) N and (f) S in N-MoS_2 electrode discharged to ~1.0 V after three cycles.

References

[1] A. O'Neill, U. Khan, J. N. Coleman, *Chem. Mater.* 2012, ***24***, 2414-2421.

[2] S. Wang, Q. Gao and J. Wang, *J. Phys. Chem. B*, 2005, **109**, 17281-17289

[3] S. Qin, W. Lei, D. Liu and Y. Chen, *Scientific Reports*, 2014, **4**, 7582

[4] H. Liu, C. Li, H. P. Zhang, L. J. Fu, Y. P. Wu and H. Q. Wu, *J. Power Sources*, 2006, **159**, 717-720.